

# SCIENTIFIC REPORTS



OPEN

## Dimethyl diallyl ammonium chloride and diallylamin Co-polymer modified bio-film derived from palm dates for the adsorption of dyes

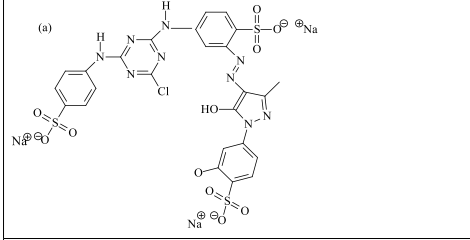
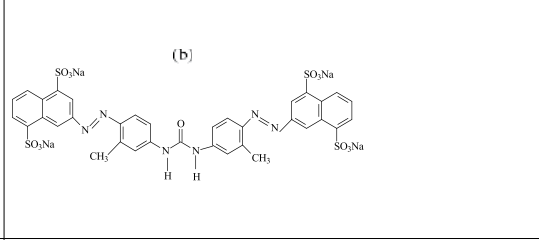
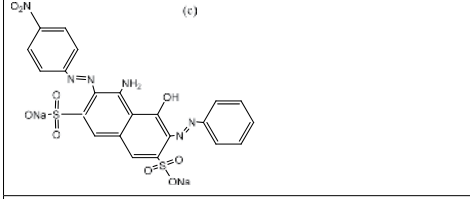
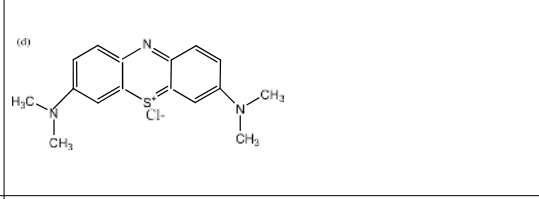
Mahjoub Jabli<sup>2,3</sup>, Tawfik A. Saleh<sup>1</sup>, Nouha Sebeia<sup>2</sup>, Najeh Tka<sup>3</sup> & Ramzi Khiari<sup>4</sup>

For the first time, co-polymer of dimethyl diallyl ammonium chloride and diallylamin (PDDACD) was used to modify the films derived from the waste of palm date fruits, which were then investigated by the purification of colored aqueous solutions. The physico-chemical characteristics were identified using data color, FT-IR spectroscopy, and SEM features. The modified films were evaluated as adsorbents of Methylene Blue (MB), Direct Yellow 50 (DY50), Reactive Blue 198 (RB198) and Naphtol Blue Black (NBB). High retention capacities were achieved in the following order: The equilibrium data  $DY50 (14 \text{ mg g}^{-1}) < RB198 (16 \text{ mg g}^{-1}) < NBB (63.9 \text{ mg g}^{-1}) < MB (150 \text{ mg g}^{-1})$ . The kinetic modeling of the data revealed that the adsorption data follows the pseudo second order model. It was fitted to the Langmuir, Freundlich, Temkin, and Dubinin-Redushkevich equations, and the data best fit the Freundlich model indicating that the adsorption might occur in the heterogeneous adsorption sites. These results reveal that PDDACD modified films are valuable materials for the treatment of industrial wastewater. Moreover, the as-prepared adsorbent is economically viable and easily controllable for pollutant adsorption.

Water contamination could lead to several harmful effects, including the destruction of aquatic life, and even have a hazardous influence on humans. As a result, the removal of pollutants is important for controlling water quality. The treatment of water by adsorption using adsorbent is one of the most promising methods. The capacity for the pollutants' removal is a function not only of the pore size and structure of the adsorbent but also depends on the molecular size and chemical nature of the solutes<sup>1</sup>. For a long time, one emergent concern has been devoted to using available low-cost materials for the removal of pollutants<sup>2,3</sup>. In this framework, previous studies bear with the development of many methods to treat polluted and colored water through sorption or degradation process<sup>4-10</sup>.

Recently, we demonstrated that 4-methyl-2-(naphthalen-2-yl)-N-propylpentanamide functionalized ethoxy-silica could be used as an efficient adsorbent to remove a wide range of dyes (acid, direct, reactive and basic) from an aqueous suspension<sup>11</sup>. In particular, the most frequent examples given were forest products that were proven to be competent and were used as adsorbents are palm ash<sup>12</sup>, rice husk<sup>13</sup>, sawdust and almond Shell<sup>14,15</sup>. Many parts of the palm plant have been extensively studied in wastewater treatment mainly trees<sup>16</sup>, leaf<sup>17</sup>, and fruits<sup>18</sup>. For example, the studies reported by Banat *et al.*<sup>19</sup> have detailed the adsorption kinetics and isotherms of methylene blue (MB) on raw and thermally activated date pits as agricultural solid waste. Walker *et al.* have concentrated on the adsorption mechanism of the removal of heavy metals and dyes from aqueous solutions using date pits as a solid adsorbent<sup>20</sup>. However, to our best knowledge, no study about the valorization

<sup>1</sup>Chemistry Department, King Fahd University of Petroleum & Minerals, Dhahran, 31261, Saudi Arabia. <sup>2</sup>Textile Materials and Research, National School of Engineering (ENIM), Monastir, 5000, Tunisia. <sup>3</sup>Laboratory of Organic Asymmetric and Homogenous Catalysis (FSM), Monastir, Tunisia. <sup>4</sup>High Institute of Technological Studies of Ksar Hellal, 4018, Monastir, Tunisia. Correspondence and requests for materials should be addressed to T.A.S. (email: [tawfikas@hotmail.com](mailto:tawfikas@hotmail.com))

	
Reactive Blue 198 (RB198) $\lambda_{\max} = 595$ nm Molecular weight (g/mol) = 882.19	Direct Yellow 50 (DY50) $\lambda_{\max} = 390$ nm Molecular weight (g/mol) = 952.81
	
Naphtol blue Black (NBB) $\lambda_{\max} = 610$ nm Molecular weight (g/mol) = 616.49	Methylene Blue (MB) $\lambda_{\max} = 664$ nm Molecular weight (g/mol) = 319.85

**Table 1.** Chemical structures of the studied dyes and their physical characteristics: (a) RB198, (b) DY50, (c) NBB and (d) MB.

	R (%)	Standard method
Cold water extractives	6.09	T207 cm-08
Hot water extractives	12.30	T207 cm-08
1% NaOH extractives	19.29	T212 om-07
Solubility in ethanol-toluene	5.84	T204 cm-07
Ash	3.46	T211 om-07
Lignin	14.23	T222 cm-99
Holocellulose	63.55	Wise <i>et al.</i> , 1946
Hemicellulose	18.14	**
$\alpha$ -cellulose	45.41	T203 cm-99

**Table 2.** The chemical composition of the obtained bio-films from the date palm. \*\*The hemicellulose content was calculated by subtracting the cellulose content from the holocellulose content.

of the film arising from the date waste was undertaken, even in its raw or modified form, for environmental or other applications.

Problems with water are expected to grow worse in the coming decades, with water scarcity occurring globally. Addressing these problems calls for new cost-effective materials and to identify robust methods for purifying water at lower cost, while at the same time minimizing the use of chemicals and the impact on the environment.

In this work, we report the co-polymer of dimethyl diallyl ammonium chloride and diallylamin modified films derived from waste palm date fruits to obtain hybrid material as an effective, stable, and efficient adsorbent for the removal of dyes. A rapid uptake rate and high adsorption capacity were observed. The results obtained in this study deliver fundamental knowledge as well as valuable experience, which will serve as a reference for the planning and design of the polymer modification of films for removing pollutants in wastewater, where chemical production, mining sites, and mine wastes are important.

## Experimental Procedure

**Chemicals and reagents.** The liquid co-polymer of dimethyl diallyl ammonium chloride and diallylamin (PDDACD) was laboratory grade. MB, RB198, DY50, and NBB were supplied from Sigma Aldrich. Their chemical structures and physical characteristics were given in Table 1. All chemical reagents were, also, purchased from Sigma Aldrich and used as laboratory grade.

**Extraction and functionalization.** The films were collected from palm dates grown from the “*Canticha*” and “*Deghla*” varieties. They were rinsed with water many times to remove the impurities deposited on the surface. The modification of the films was performed at a temperature of 50 °C for 30 mins in the presence of NaOH (2%) within a range of 0.05–5% PDDACD according to the process described in Fig. 1. PDDACD, with the structure drawn in Fig. 1, was added to the films and well mixed. Then, 2% NaOH solution was dropwise added and the mixture was stirred for 30 mins, followed by cooling. Then, the mixture was neutralized by acetic acid which was followed by washing with distilled water. Figure 2 depicts the structure of poly-dimethyl-diallyl-ammonium-chloride-diallylamin-co-polymer (PDDACD). Figure 3 depicts the proposed

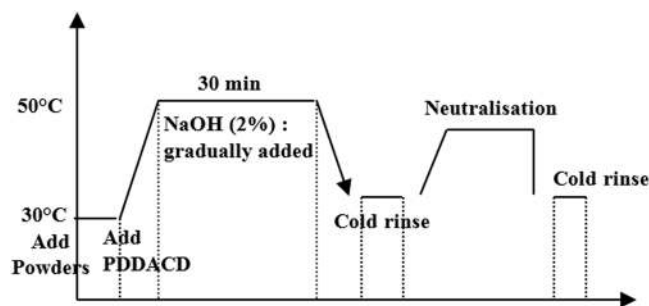


**Figure 1.** Cationization process using PDDACD.

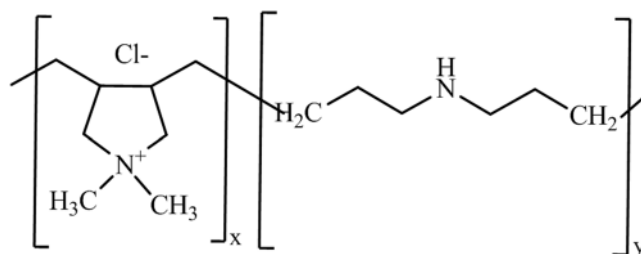


**Figure 2.** Structure of poly-dimethyl-diallyl-ammonium-chloride-diallylamin-co-polymer (PDDACD).

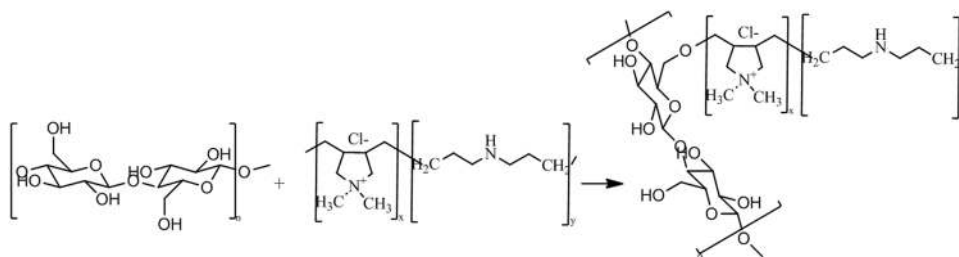


**Figure 3.** A proposed mechanism of interaction between cellulose chains of raw film and PDDACD.

N°	<i>Kanticha</i> variety			<i>Deghla</i> variety		
	L*	a*	b*	L*	a*	b*
1	64.69	1.14	7.79	70.27	1.12	11.16
2	67.58	0.81	8.61	68.85	1.59	12.03
3	67.56	1.24	10.18	69.88	2.05	13.23
4	66.72	1.63	10.75	70.49	1.5	10.91
5	68.27	1.14	10.43	68.89	1.27	11.25
6	68.94	0.99	9.71	69.9	2.2	13.28
7	68.71	0.82	9.27	67.08	2.14	13.05
8	68.49	1.11	10.09	70.73	1.78	11.9
9	69.47	0.72	8.65	69.26	1.75	10.66
10	69.71	1.19	9.99	67.63	2.48	13

**Table 3.** Color coordinates for *Kanticha* and *Deghla* varieties.

chemical structure of the obtained dimethyl diallyl ammonium chloride and diallylamin co-polymer modified bio-film.

The obtained raw materials were ground and 40–60 mesh fractions were selected according to the standard procedures T264 cm-07 to determine their chemical composition. The chemical analysis of the film obtained from date palm was performed according to the standard methods. The evaluation of the extractive substances was carried out in various liquids according to common standards. The solubility in hot and icy water, 1% NaOH and in ethanol–toluene was established according to the TAPPI standards methods: T207 cm-08, T212 om-07,

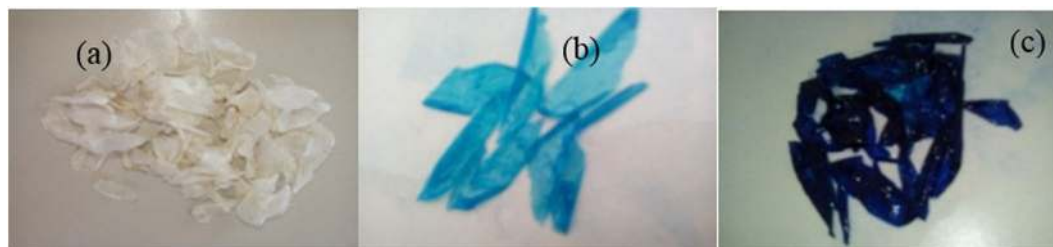


**Figure 4.** Photos of (a) residual films (b) after contact with MB [10 mg/L] and (c) [30 mg/L].

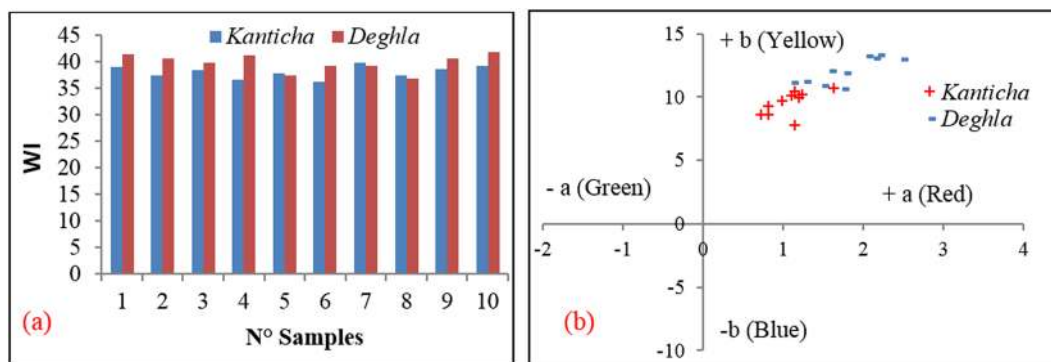


**Figure 5.** Variation of: (a) WI for films from the Kanticha and *Deghla* varieties and (b) evolution of their yellowish and reddish color.

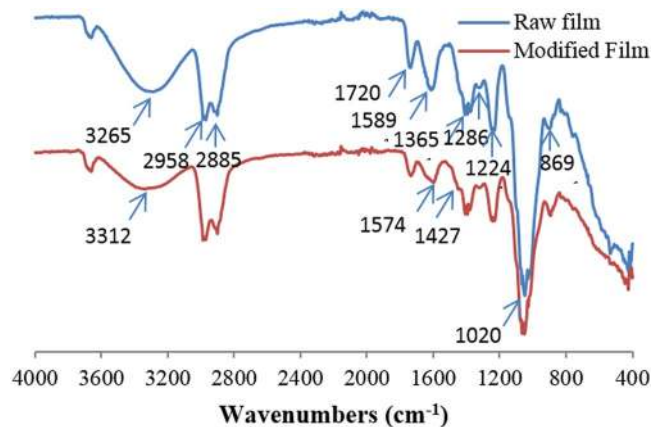


**Figure 6.** FT-IR spectra of raw and modified film.

and T204 cm-07 respectively. The ash amount was established according to standard T211 om-07. The quantities of lignin, holocellulose and  $\alpha$ -cellulose, were also evaluated using the following respective TAPPI standard methods: T222 om-06, the method of Wise *et al.*<sup>21</sup> and T203 cm-99. All the experiments were duplicated and the difference between the values was within an experimental error of 5%.

**Characterization.** An FT-IR apparatus (PerkinElmer 100 spectrometer, USA) was used to determine the different function groups present in the structure of film palm date waste after chemical modification. In order to obtain a good resolution of the spectrum, the spectra of the samples were obtained after 32 scans from 400 to 4000  $\text{cm}^{-1}$  with a resolution of 4  $\text{cm}^{-1}$ .

The morphological features of the products before and after modification were analyzed using the SEM apparatus (Hitachi S-2360N). Samples were previously coated with gold using a vacuum sputter-coater in order to improve their conductivity and the quality of the SEM images. The accelerating voltage was equal to 20 kv. A spectrophotometer was employed to measure the absorbance value of dyes before and after adsorption. The whiteness index and the color coordinates of raw films were assessed using a data color instrument.

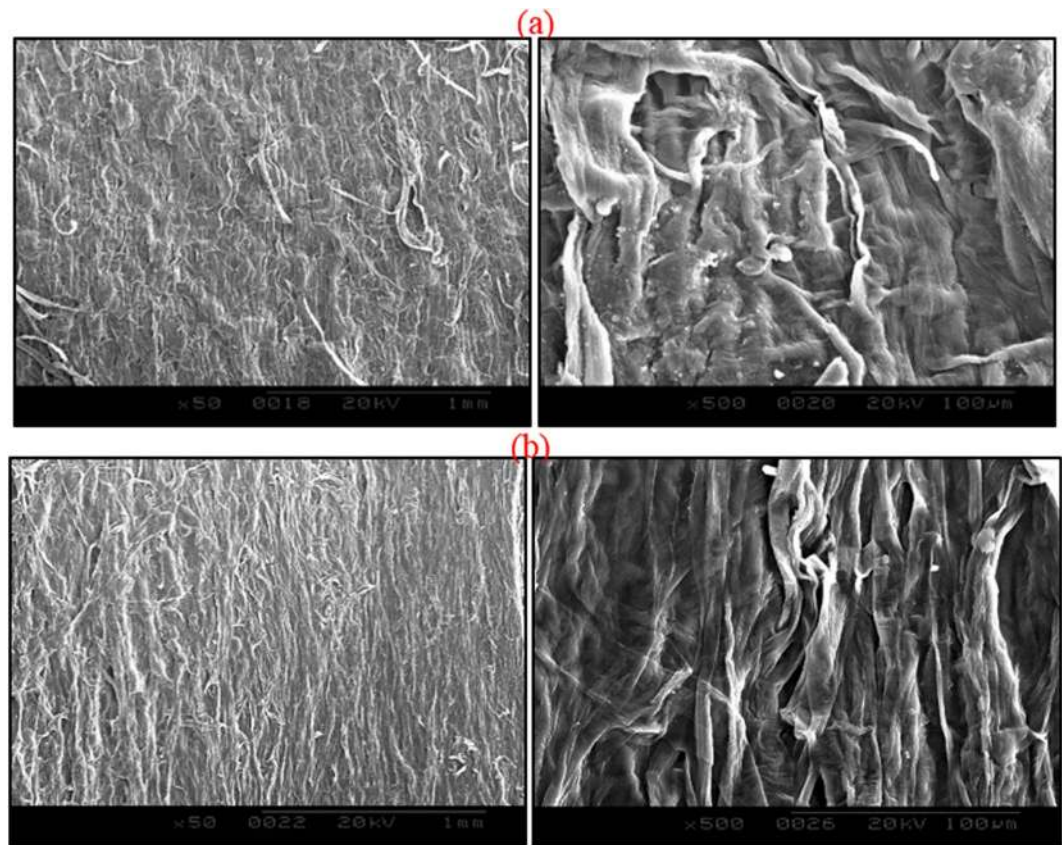


**Figure 7.** Micrograph of (a) unmodified and (b) modified films ( $\times 50$  and  $500$ ).

**Adsorption experiments.** Kinetic studies were carried out by agitating a series of flasks containing 50 mL of dye solutions of an initial concentration of  $30 \text{ mg.L}^{-1}$  with 0.05 g amount of adsorbent (unmodified and modified film waste) with a constant agitation speed (50 rpm). Agitation was provided for 4 h after which equilibrium was reached, Fig. 4. After reaching an equilibrium state, the contents were filtered to separate the adsorbents from the suspension using a sintered glass. The pH values were ranged from 3 to 9 at temperatures from 25 to  $60^\circ\text{C}$  to examine the effect of the experimental conditions on the adsorption phenomenon. All the experiments were duplicated and the difference between the values was within the experimental error of 5%.

## Results and Discussion

**Chemical analysis.** The average results of the chemical analysis of the bio-films obtained from date palm were determined (Table 2). It was registered that the starting raw material was characterized by relatively high amounts of 12.3% in hot water and 6.09% in cold water extractives. Extractions were carried out under alkaline conditions which yielded a very high content, i.e. 20%, which probably indicates oligosaccharide and lignin-rich materials<sup>22,23</sup>. The ash content is equal to 3.46%. Whereas the ethanol-toluene extractives (5.84%), holocellulose (63.55%) and  $\alpha$ -cellulose contents (45.41%) are comparable to those of other annual plants or agricultural crops<sup>24</sup>. Klason lignin was found to be relatively lower (14.23%). The polysaccharide content is close to that associated with wood materials, which makes the waste a very promising candidate to investigate for the isolation of cellulose as composite materials and/or papermaking, and/or as a substrate for cellulose derivatives.

**Physical characteristics.** The major produced varieties of palm date in Tunisia are namely: Deghla, Kenticha, Alig, KentaGenda and Kosbi differentiated by the aspect of their fruit. Herein, the WI variation of the raw films for two abundant varieties, Kanticha and deghla, in our region (Sidi Bouzid, Tunisia) was measured in order to examine variations in the native color. From Fig. 5a, only a slight change in the WI value inside the whole variety is observed. In fact, the WI values varied from 36.2 to 39 and from 36.7 to 42 for Kanticha and Deghla, respectively. Applying the equation 1, the Cv (%) allows us to comment on the homogeneity of the serial of each variety. This value was found to be equal to 2.06% and 1.65% for the Kanticha and Deghla varieties, respectively.

$$CV (\%) = \frac{\sqrt{\frac{1}{n}(X_i - M)^2}}{M} \quad (1)$$

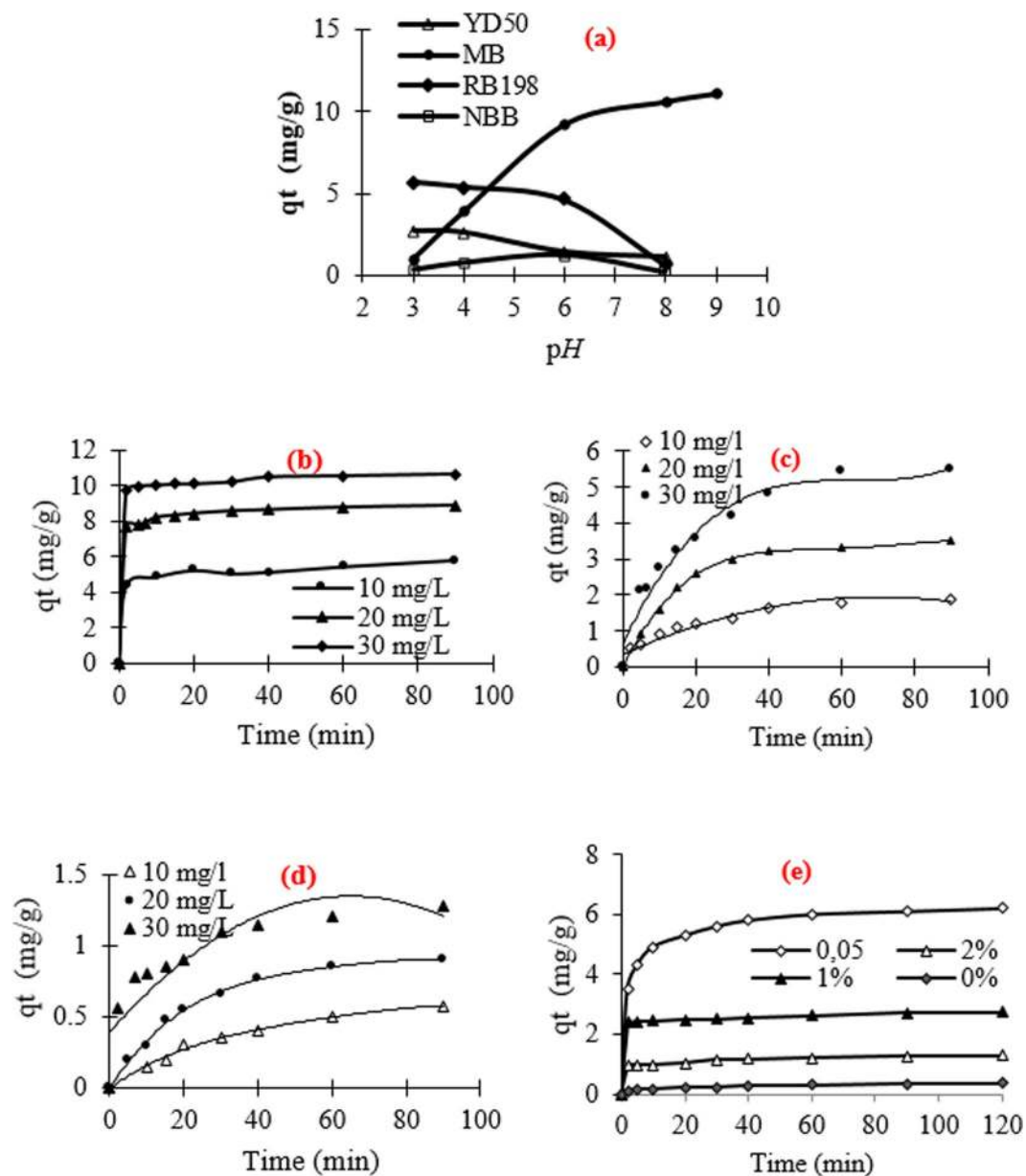


**Figure 8.** (a) Effect of pH on the adsorption of dyes ( $c_0 = 30$  mg/L,  $t = 1$  h,  $T = 25^\circ\text{C}$ ), Change of  $q_t$  against time for the adsorption of: (b) MB, (c) RB198, (d) DY50 and (e) NBB ( $T = 25^\circ\text{C}$ ,  $\text{pH} = 6$ ,  $c_0 = 30$  mg/L) on the surface of bio-films.

Contrary to *Deghla*, the *Kanticha* variety bears a dry fruit in nature and consequently, the bio-films could be easily separated from the date waste. As a result, it was selected as a candidate for further dye sorption experiments.

The color parameters ( $L^*$ ,  $a^*$  and  $b^*$ ) were, also, assessed and the results were tabulated in Table 3. The  $L^*$  parameter is associated with the lightness of the color and moves from the top (value: 100, white) to bottom (value: 0, black). For the studied films, it varies between 69.71 and 64.69 CIELAB units indicating a perceptible brightness in the studied films. The value of  $a^*$  [associated with greenness (–) to redness (+) changes] varied from 0.72 to 1.63, conferring the products with a reddish color. The changes in  $b^*$  [associated with blueness (–) to yellowness (+) changes] ranges from 7.79 to 10.75, conferring the products with a yellowish color. The comparison between the *Kanticha* and *Deghla* varieties reveals that the latter is more red and yellow in color.

**FT-IR investigations.** The FT-IR spectra of raw and functionalized films are given in Fig. 6. The results depicted that the raw film showed a strong broad band at around  $3265\text{ cm}^{-1}$  corresponding to the OH stretching mode. The cellulose structure of the film is confirmed by the presence of many characteristic bands: the peak at  $869\text{ cm}^{-1}$  (an amorphous region in cellulose) is assigned to  $\beta$ -glucosidic linkages<sup>25</sup>. The band at  $1020\text{ cm}^{-1}$  is attributed to the C-OH stretching vibration of the cellulose backbone ( $\nu$ C-O secondary alcohol)<sup>26</sup>. The symmetric

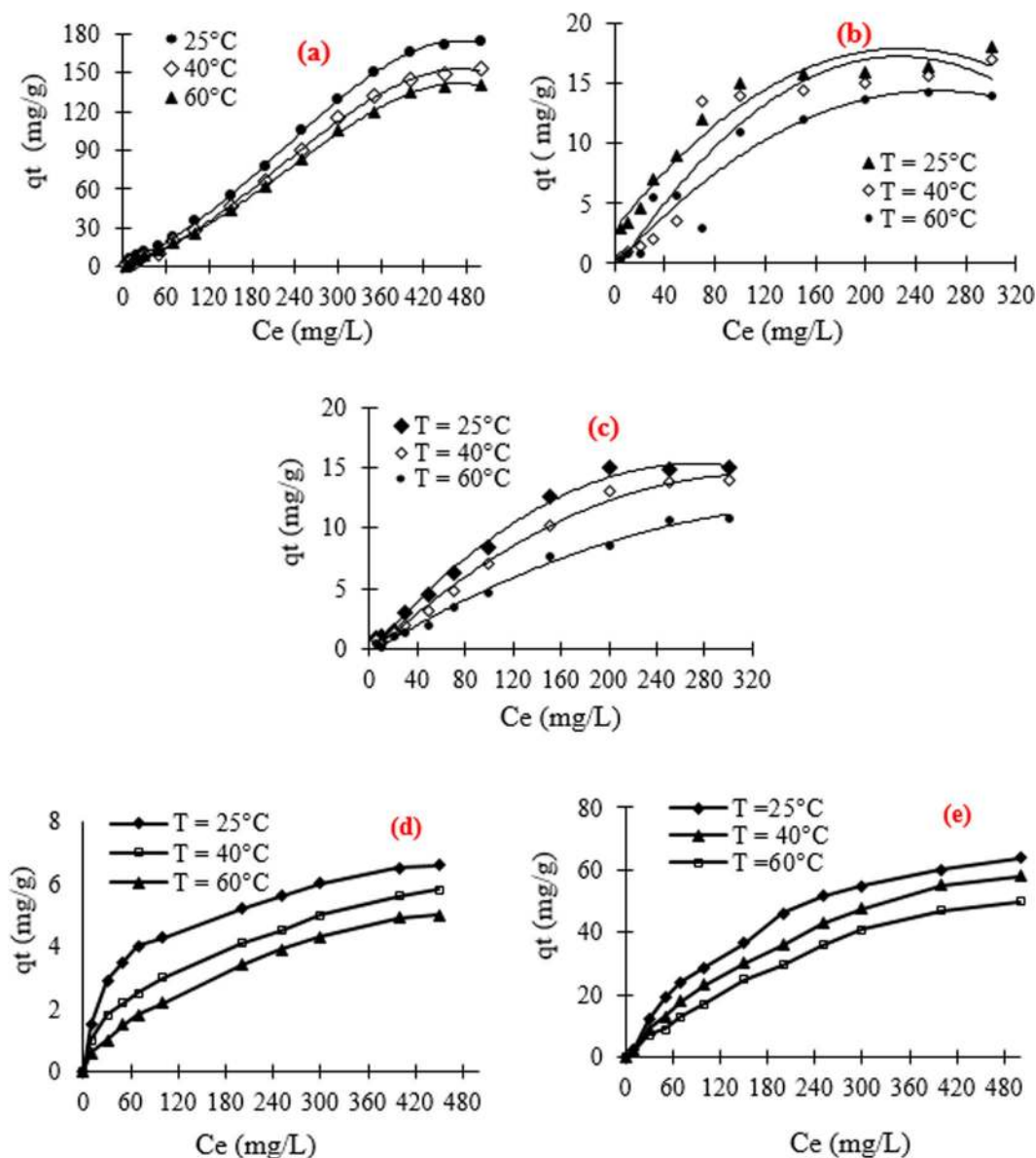


**Figure 9.** Evolution of  $q_t$  versus  $C_e$ : (a) MB, (b) RB198, (c) DY50, (d) Variation of temperature for NBB Unmodified film and (e) Variation of temperature for NBB cationized film.

CH bending of the methoxyl groups was observed at  $1365\text{ cm}^{-1}$ <sup>27</sup>. The two bands at around  $2885$  and  $2958\text{ cm}^{-1}$ , are related to  $-\text{OCH}_3$  methoxyl C-H stretching and C-H stretching groups<sup>28,29</sup>. The peaks present at  $1720$  ( $\text{C}=\text{O}$  linkage) and  $1224\text{ cm}^{-1}$  (aromatic skeletal vibration) are characteristic groups of lignin and hemicelluloses<sup>30</sup>. The bands at  $1589$  and  $1286\text{ cm}^{-1}$  are assigned to  $\text{C}=\text{C}$  and  $\text{C}-\text{O}$  stretching vibrations of different groups present in lignin<sup>28</sup>.

Compared with the IR spectrum of raw film, the spectrum of the modified film exhibits the shifting of the band at  $3265\text{ cm}^{-1}$  (OH stretching groups) to  $3312\text{ cm}^{-1}$ . This confirms the addition of ammonium ions arising from the PDDACD structure. It can be also observed that there is an appearance of two new peaks at  $1427$  and  $1574\text{ cm}^{-1}$  which are attributed to the C-N stretching vibration and N-H in the secondary amine ( $-\text{NH}$ ), respectively<sup>31</sup>. These results corresponded to the quaternary ammonium salt groups which reacted on the cellulose backbone.

**SEM characterization.** The morphological features of the films were examined by Scanning Electron Microscopy and the results were given in Fig. 7. The SEM image (Fig. 7a) shows a micrograph of the unmodified films waste surface where a system of shallow parallel grooves is observed. Figure 7b depicts the micrographs of the film-PDDACD surface. It can be concluded, based on these micrographs, that there are no clear changes in surface morphology and the cationized surfaces are slightly smoother than that of the unmodified films. It can be concluded that the cationization does not alter the fiber's physical structure. This is an advantage of the treatment compared to some other polymer material treatments (i.e. chitosan) which produce a degree of stiffness.

Samples	$q_m$ (mg.g <sup>-1</sup> )	References
Almond Shell waste	84.9	36
Hydroxyapatite	98.23	37
Zeolite ZK	21.41	38
SDBS-modified ZSM-5	15.68	38
Hydroxysodalite	10.82	38
Elaeagnus angustifolia	75,75	39
Pyrolytic tire Char	50	40
Bio-films from palm date	150	Current study

**Table 4.** The maximum adsorption capacities (mg.g<sup>-1</sup>) of MB from the literature by other adsorbents.

$C_0$ (mg/L)	Pseudo-first-order				Pseudo-second-order				Elovich			Diffusion	
	$K_1$	$q_e$	$R^2$	SSE	$K_2$	$q_e$	$R^2$	SSE	$\alpha$	$\beta$	$R^2$	$K_1$	$R^2$
<b>MB</b>													
10	0.0089	2.135	0.66	0.461	0.093	5.76	0.99	0.009	6.654	0.657	0.623	0.4059	0.511
20	0.01	1.891	0.55	0.87	0.003	8.888	0.99	0.002	28.58	0.754	0.529	0.586	0.412
30	0.0098	1.829	0.48	1.1	0.153	10.66	0.99	0.002	303.6	1.119	0.475	0.6697	0.366
<b>RB198</b>													
10	0.007	1.824	0.9	0.006	0.054	2.014	0.97	0.017	0.468	2.493	0.975	0.1988	0.952
20	0.0098	2.9	0.86	0.075	0.099	3.852	0.97	0.044	0.778	1.207	0.971	0.4009	0.904
30	0.0119	4.301	0.92	0.146	0.021	5.875	0.97	0.05	1.656	0.883	0.944	0.564	0.93
<b>DY50</b>													
10	0.0028	1.213	0.94	0.079	0.049	0.724	0.85	0.018	0.068	7.553	0.913	0.0657	0.98
20	0.0038	1.39	0.85	0.06	0.058	1.055	0.94	0.019	0.143	4.57	0.957	0.1042	0.95
30	0.0038	1.376	0.71	0.012	0.14	1.32	0.99	0.0005	0.453	3.731	0.937	0.12	0.83
<b>NBB</b>													
0%	0.003	0.494	0.838	0.015	0.356	0.378	0.983	0.002	0.11	13.568	0.97	0.036	0.926
0.05%	0.009	2.452	0.801	0.416	0.078	6.305	0.999	0.011	5.2	0.8579	0.82	0.099	0.585
1%	0.005	0.82	0.472	0.212	0.342	2.74	0.999	0.001	9.09	2.504	0.52	0.179	0.416
2%	0.004	0.494	0.621	0.088	0.373	1.309	0.998	0.002	1.84	4.697	0.69	0.529	0.672

**Table 5.** Summarized kinetic constants for the adsorption of different dyes on the surface of unmodified and cationized films.

**Adsorption of dyes on unmodified and modified films.** The interaction of film chains with the studied representative adsorbates is conditioned, not only by the presence of functional groups on the surface of either the adsorbent or the adsorbate but also by several experimental parameters including pH value, duration of contact, initial adsorbate concentration, temperature range, etc.

**Effect of pH value.** The effect of pH on the adsorption of DY50, MB, RB198, and NBB is given in Fig. 8a. The adsorption capacity achieved its maximum at pH 4 for RB198 and DY50, pH 8 for BM and pH 6 for NBB. For example, for MB, the adsorption capacity increases from 1 to 10.5 mg.g<sup>-1</sup> when the pH ranges from 3 to 9. These lower  $q_t$  values observed for MB, at an acidic pH, might be due to the presence of excess H<sup>+</sup> ions competing with dye cations for the available adsorption sites<sup>32</sup>. The results agree with other reports studying the removal of MB on aluminum industry waste and on low-cost activated carbon derived from agricultural waste material, respectively<sup>2,33</sup>.

**Effect of time.** The variation of the adsorbed quantity of the film waste versus time is given in Fig. 8b–e. As globally observed, the sorption equilibrium was rapidly achieved for dye concentrations ranging from 10 to 30 mg.g<sup>-1</sup>. Indeed, only 5 minutes of contact adsorbent-MB were sufficient to achieve equilibrium, 40 minutes for RB198 and 80 minutes for DY50. This difference in the rate and capacity of sorption is explained based on the reactivity of the film wastes, the molecular weight and the nature of the dye itself (Table 1). In addition, the functionalization with PDDACD was found to enhance significantly the adsorption of NBB. The adsorbed amount is about 5.9 mg.g<sup>-1</sup> ( $C_0 = 30$  mg.L<sup>-1</sup>) for the optimum dose of PDDACD (0.05%). However, it does not exceed 0.25 mg.g<sup>-1</sup> for the raw film under the same conditions. In addition, it can also be noticed that the adsorbed amount of NBB decreases with the increase in the cationic agent dose. For example,  $q_t$  decreases from 5.9 mg.g<sup>-1</sup> (optimum dose of PDDACD) to 1.29 mg.g<sup>-1</sup> for the same experimental conditions using a high cationic dose equal to 2%. The trend in capacity removal  $q_t$  can be explained by the effect of an ionic attraction between the PDDACD cationic groups and the dye anionic groups. Nevertheless, for modified films,  $q_t$  is slightly reduced at high doses of the cationic agent. These trends are due to the formation of the dye-PDDACD complex on the film



T (°C)	Langmuir			Freundlich			Temkin			Dubinin				
	q <sub>m</sub>	R <sup>2</sup>	SSE	K <sub>F</sub>	n	R <sup>2</sup>	B	A <sub>t</sub>	R <sup>2</sup>	qm	E	R <sup>2</sup>	SSE	
<b>RB198</b>														
25	16.52	0.81	0.41	0.392	1.505	0.781	2.955	0.2	0.946	7.0766	40.8	0.84	0.447	
40	17.85	0.81	0.67	0.177	1.292	0.924	2.834	0.13	0.9609	5.2221	19.6	0.718	0.47	
60	20.242	0.696	1.022	0.1	1.202	0.97	2.443	0.1	0.9092	3.632	28.9	0.63	0.488	
<b>MB</b>														
25	48.309	0.728	8.379	0.022	1.148	0.985	4.811	0.12	0.89	5.8814	18.9	0.535	11.2	
40	51.282	0.78	6.781	0.009	1.113	0.995	4.19	0.11	0.896	6.0122	21.3	0.641	9.79	
60	25.188	0.917	7.72	0.004	1.141	0.992	2.564	0.12	0.9	4.1768	35.4	0.739	9.12	
<b>DY50</b>														
25	48.309	0.728	2.02	0.193	1.148	0.985	4.811	0.12	0.89	5.8814	18.9	0.535	0.8	
40	39.215	0.637	1.614	0.136	1.13	0.977	3.752	0.13	0.88	5.6933	28.9	0.657	0.7	
60	23.809	0.739	0.92	0.091	1.139	0.983	2.329	0.15	0.8684	3.8098	50	0.737	0.41	
<b>NBB: Unmodified film</b>														
25	7.132	0.057	0.997	0.053	1.243	2.939	0.89	1.359	0.929	0.98	5.092	25	0.876	0.15
40	6.707	0.029	0.99	0.09	0.595	2.211	0.94	1.3	0.348	0.98	4.211	28.86	0.805	0.158
60	6.215	0.02	0.979	0.12	0.319	1.833	0.94	1.247	0.256	0.97	3.364	40.824	0.741	0.16
<b>NBB: Modified film</b>														
25	84.74	0.014	0.87	2.085	2.067	1.44	0.84	15.52	0.238	0.98	38.08	17.149	0.927	2.58
40	86.2	0.009	0.77	2.82	1.478	1.401	0.87	14.78	0.171	0.98	35	21.32	0.895	2.29
60	75.18	0.008	0.79	2.52	1.266	1.432	0.89	12.23	0.172	0.95	26.46	35.355	0.704	2.35
<b>Thermodynamic parameters</b>														
	T (°C)	$\Delta H^*$ (KJ.mol <sup>-1</sup> )			$\Delta S^*$ (J.mol <sup>-1</sup> )			$\Delta G^*$ (KJ.mol <sup>-1</sup> )						
		25	40	60	25	40	60	25	40	60				
Unmodified film	RB198	-28.255			-132			11.294 13.285 15.939						
	DY50	-0.117			-47			14.149 15.825 15.825						
	NBB	-24.152			-105			7.273 8.855 10.964						
	MB	-0.389			-50			14.744 15.506 16.521						
Functionalized film	NBB	-12.071			76			10.804 11.956 13.491						

**Table 6.** Summarized constants values of Langmuir, Freundlich, Temkin, and Redushkevich for the adsorption of the different dyes on the surface of raw and cationized films. Thereafter, the thermodynamic parameters  $\Delta H^\circ$  and  $\Delta S^\circ$  were computed from the slope and the intercept of the linear plot of  $\ln Kf$  vs.  $1/T$  (Figure S5) and the results are summarized in Table 6. It can be observed that the enthalpy values are negative. This suggests that the interaction of the four studied dyes within the film is exothermic. This result agrees well with both the decrease in the capacity removal with temperature values and with the decrease of the adsorption energy constants (B) calculated from the Temkin equation. The positive values of  $\Delta G^*$  and negative values of  $\Delta S^*$  means the non-spontaneous reaction and the decrease of the disorder, respectively. However, in the case of the adsorption of NBB using functionalized films as adsorbents, the cationization allows for the increase in the disorder of the system (Table 6).

waste surface which, because of steric hindrance, blocks dye diffusion through functional hydroxyl groups into the cellulosic film. Similar behaviors were also observed in the reports by Mouxiou *et al.*<sup>34</sup> when studying the cationic surfactants and their interaction with reactive dyes and during the investigation of Nebojša Ristić *et al.*<sup>35</sup> which describes the cationic modification of cotton fabrics and reactive dyeing characteristics.

**Effect of temperature.** The evolution of the adsorbed amount of MB, RB198, DY50 and NBB (Fig. 9) on the surface of the unmodified and functionalized films is studied as a function of temperature in order to comment on the exothermicity or endothermicity of the process. As depicted for the four investigated dyes, the adsorption process using film waste as adsorbent follows an exothermic mode in the range of 25–60 °C. As an example, at room temperature, when the  $C_e$  of MB increases from 5 to 500 mg.L<sup>-1</sup>, the adsorbed amount of dye achieved its maximum at about 150 mg.g<sup>-1</sup>. The maximum adsorbed quantities, at 25 °C, are to be 16 mg.g<sup>-1</sup> and 14 mg.g<sup>-1</sup> for RB198 and DY50, respectively.

The increase in the  $C_e$  values exhibits that the  $q_e$  increases from 6.6 mg.g<sup>-1</sup> for the unmodified film (Fig. 9d) waste to 63.9 mg.g<sup>-1</sup> after its functionalization with PDDACD. This proves the efficiency to modify the cellulosic chains using this cationic copolymer in the removal of anionic dyes. As globally observed for all dyes, the high capacity removal proves that this low-cost agricultural waste could be considered as an efficient adsorbent. These sorption amounts follow the order: DY50 (14 mg.g<sup>-1</sup>) < RB198 (16 mg.g<sup>-1</sup>) < NBB (63.9 mg.g<sup>-1</sup>) < MB (150 mg.g<sup>-1</sup>). This difference in capacity removal was explained by the functional groups present in the structure of each dye and their molecular weight. Indeed, DY50 and RB198 exhibited high MW values (>882 g.mol<sup>-1</sup>).

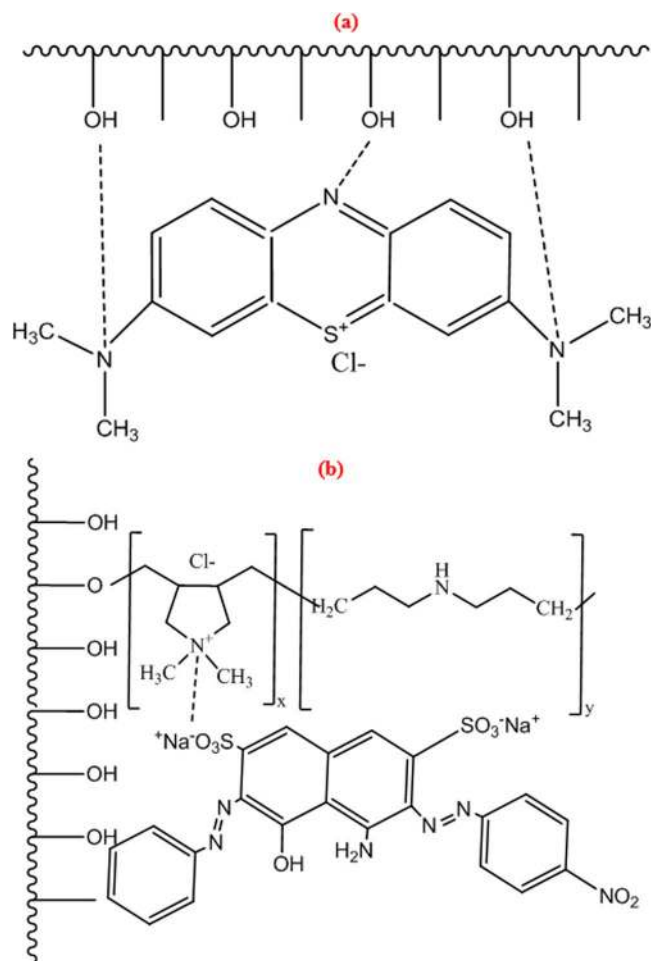


**Figure 10.** Proposed mechanism of interaction between (a) MB and raw film chains and (b) cationized film chains and NBB.

The registered maximum adsorption capacity for the removal of MB using raw films ( $150 \text{ mg.g}^{-1}$ ) as the adsorbent is compared to other adsorbents gathered from the literature (Table 4). This amount of MB removal is so very interesting and thus the studied bio-films could be seen as a good adsorbent. In fact, this value is more important compared to hydroxyapatite modified with  $\lambda$ -Carraghenan ( $98.23 \text{ mg.g}^{-1}$ ), Almond Shell waste ( $84.9 \text{ mg.g}^{-1}$ ) and *Elaeagnus angustifolia* ( $75.75 \text{ mg.g}^{-1}$ ). It is three times higher compared to Pyrolytic tire Char ( $50 \text{ mg/g}$ ). It is seven times more important than the zeolite ZK ( $21.41 \text{ mg.g}^{-1}$ ). It is nine times important than SDBS-modified ZSM-5 ( $15.68 \text{ mg.g}^{-1}$ ) and it is also fourteen times important than hydroxysodalite ( $10.82 \text{ mg.g}^{-1}$ ).

**Kinetic modeling.** The correlation of the experimental kinetic data with theoretical equations allows us to better understand the mechanism of the retention of all the studied dyes on the surface of unfunctionalized and functionalized film wastes during the sorption phenomenon. The detailed linear forms of these equations were given in the previous works<sup>10</sup>. In the present work, experimental data are discussed based on the coefficient regression  $R^2$  and the calculated SSE values (Table 5). As globally observed, for all the studied dyes using unfunctionalized (Figure S1) and functionalized film (Figure S2) waste as adsorbents, the values of  $R^2$  are found to be more important, along with the pseudo second order equation ( $R^2 > 0.85$ ) compared to the pseudo-first-order. This was also confirmed by the fact that the calculated  $q_e$  values for the pseudo-second-order kinetic model show good agreement with the experimental  $q_e$  values ( $0.0005 < \text{SSE} < 0.044$ ).

**Analysis of isotherms via Langmuir, Freundlich and Temkin and Dubinin.** The adsorption isotherms allow us to predict the feasibility of the adsorption phenomenon and represent the mechanism for the interaction between the adsorbent and the adsorbates at the studied temperatures.

Table 6 gives the different parameters gathered from the linearized data throughout Langmuir, Freundlich, Temkin, and Dubinin. The relatively low correlation coefficients show that the Langmuir isotherm (Figure S3) has a poor agreement with the experimental data which suggests that the adsorption phenomenon does not occur on a single surface. On the contrary, the Freundlich isotherm fits the experimental data quite well with high correlation coefficients ( $R^2 > 0.78$ ) for the four studied dyes. The consistency of the Freundlich isotherm with the data reveals that the adsorption might occur in the heterogeneous adsorption sites. However, the adsorption of NBB (Figure S4) on raw films could be described by the Langmuir equation. As globally observed, the studied fibers

are moderate adsorbents ( $1 < n < 2$ ) for the four studied dyes but poor sorbents for NBB ( $n < 1$ ) in the case of the unfunctionalized film at temperatures higher than the ambient<sup>8,41–45</sup>.

**Immobilization mechanism.** Indeed, the film chains could interact with the MB molecules via the hydrogen bonding mode through the presence of nitrogen atoms and hydroxyl groups in the structure of MB and cellulosic chains, respectively, Fig. 10(a). On the other hand, after cationisation, the ionic ammonium added on the surface of cellulosic chains might react with NBB via ionic interactions between the  $N^+$  and the  $SO_3^-$  groups, Fig. 10(b).

## Conclusions

In summary, we have developed a new adsorbent which consists of a co-polymer of dimethyl diallyl ammonium chloride and diallylamin modified films derived from the waste of palm dates. The hybrid material showed efficient removal of dyes from polluted water. The good stability, fast adsorption rate, high adsorption capacity, and excellent pH tolerance were validated by using a batch separation mode. The capacities removal follows the order: DY50 ( $14 \text{ mg.g}^{-1}$ ) < RB198 ( $16 \text{ mg.g}^{-1}$ ) < NBB ( $63.9 \text{ mg.g}^{-1}$ ) < MB ( $150 \text{ mg.g}^{-1}$ ). The pseudo-second-order was adequate to describe the experimental data. The modeling of the isotherms reveals that the Langmuir model is more suitable to describe the adsorption data. The values of the thermodynamic parameters suggest that the phenomenon is exothermic with a non-spontaneous reaction. Moreover, the results from the chemical composition investigation exhibited that the polysaccharide content is similar to that associated with wood materials, which supports the conclusion that the films have the potential to isolate cellulose as composites, for papermaking and as a substrate for cellulose derivatives, and can thus be utilized for a wide range of applications.

## References

- Kyzas, G. Z. & Kostoglou, M. Green Adsorbents for Wastewaters: A Critical Review. *Materials* **7**, 333–364 (2014).
- Gupta, V. K., Ali, I. & Saini, V. K. Removal of rhodamine B, fast green, and methylene blue from wastewater using red mud, an aluminum industry waste. *Industrial Engineering Chemical Research* **43**, 1740–1747 (2004).
- Saleh, T. A. Mercury sorption by silica/carbon nanotubes and silica/activated carbon: a comparison study. *Journal of Water Supply: Research and Technology-Aqua* **64**(8), 892–903 (2015).
- Jabli, M., Baouab, M. H. V., Roudesli, M. S. & Bartegi, A. Adsorption of Acid Dyes from Aqueous Solution on a Chitosan-cotton Composite Material Prepared by a New Pad-dry Process. *Journal of Engineered Fibers and Fabrics* **6**, 1–12 (2011).
- Jabli, M., Aloui, F. & Ben Hassine, B. [Copper (II)/Cellulose-Chitosan] Microspheres Complex for Dye Immobilization: Isotherm, Kinetic and Thermodynamic Analysis. *Journal of Engineering Fibers and Fabrics* **8**, 19–34 (2013).
- Gupta, V. K. *et al.* Photo-catalytic degradation of toxic dye amaranth on  $TiO_2/UV$  in aqueous suspensions. *Materials Science and Engineering C* **32**, 12–17 (2012).
- Mittal, A., Mittal, J., Malviya, A., Kaur, D. & Gupta, V. K. Decoloration treatment of a hazardous triarylmethane dye, Light Green SF (Yellowish) by waste material adsorbents. *Journal of Colloid and Interface Science; Volume* **342**, 518–527 (2010).
- Mittal, A., Kaur, D., Malviya, A. & Gupta, V. K. Adsorption studies on the removal of coloring agent phenol red from wastewater using waste materials as adsorbents. *Journal of Colloid and Interface Science* **337**, 345–354 (2009).
- Mittal, A., Mittal, J., Malviya, A. & Gupta, V. K. Adsorptive removal of hazardous anionic dye “Congo red” from wastewater using waste materials and recovery by desorption. *Journal of Colloid and Interface Science* **340**, 16–26 (2009).
- Gupta, V. K. *et al.* Chemical treatment technologies for waste-water recycling—an overview. *RSC Advances* **2**, 6380–6388 (2012).
- Jabli, M., Baccouch, W., Hamdaoui, M., Aloui, F. & Ben Hassine, B. Removal of a wide range of dyes using 4-methyl-2-(naphthalen-2-yl)-N-propylpentanamide-functionalized ethoxy-silica and raw silica. *Journal of Textile Institute* **108**(2), 1–11 (2016).
- Saleh, T. A. *Advanced Nanomaterials for Water Engineering, Treatment, and Hydraulics* (Advances in Environmental Engineering and Green Technologies), (first ed.), IGI Global (2017), ISBN-13: 978-1522521365.
- Malik, P. K. Use of activated carbons prepared from sawdust and rice-husk for adsorption of acid dyes: a case study of Acid Yellow 36. *Dyes and Pigments* **56**(3), 239–249 (2003).
- Al-Amoudi, O., Al-Homidy, A. A., Maslehuddin, M. & Saleh, T. A. Method and Mechanisms of Soil Stabilization Using Electric Arc Furnace Dust. *Scientific Reports* **7**, 46676 (2017).
- Ismail, O. E., Yildirim, L. & Özdoğan, E. Use of almond shell extracts plus biomordants as effective textile dye. *Journal of Cleaner Production* **70**, 61–67 (2014).
- Belala, Z., Jeguirim, M., Belhachemi, M., Addoun, F. & Trouvé, G. Biosorption of basic dye from aqueous solutions by date Stones and Palm-Trees Waste: Kinetic, equilibrium and thermodynamic studies. *Desalination* **271**(1–3), 80–87 (2011).
- El-Shafey, E. I., Ali, S. N. F., Al-Busafi, S. & Al-Lawati, H. A. J. Preparation and characterization of surface functionalized activated carbons from date palm leaflets and application for methylene blue removal. *Journal of Environmental Chemical Engineering* **4**(3), 2713–2724 (2016).
- Azharul Islam, M. D., Tan, I. A. W., Benhouria, A., Asif, M. & Hameed, B. H. Mesoporous and adsorptive properties of palm date seed activated carbon prepared via sequential hydrothermal carbonization and sodium hydroxide activation. *Chemical Engineering Journal* **270**, 187–195 (2015).
- Banat, F., Al-Asheh, S. & Al-Makhadmeh, L. Evaluation of the use of raw and activated date pits as potential adsorbents for dye containing waters. *Process Biochemistry* **39**(2), 193–202 (2003).
- Walker, G. & Ahmad, M. N. M. Adsorption mechanisms of removing heavy metals and dyes from aqueous solution using date pits solid adsorbent. *Journal of Hazardous Materials* **176**(1–3), 510–520 (2010).
- Wise, L. E., Murphy, M. & D’Addieco, A. A. Chlorite holocellulose: its fractionation and bearing on summative wood analysis and on studies on the hemicellulose. *Paper Trade Journal* **122**(2), 35–43 (1946).
- Khiari, R., Mhenni, M. F., Belgacem, M. N. & Mauret, E. Chemical composition and pulping of date palm rachis and *Posidonia oceanica* - A comparison with other wood and non-wood fibre sources. *Bioresource Technology* **101**, 775–780 (2010).
- Mansouri, S. *et al.* Chemical composition and pulp characterization of Tunisian vine stems. *Industrial Crops and Products* **36**, 22–27 (2012).
- Mechi, N., Khiari, R., Ealoui, L. & Belgacem, M. N. Preparation of paper sheet from cellulosic fibres obtained from *Prunus amygdalus* and *Tamarisk* sp. *Cellulose Chemistry and Technology* **7**(8), 863–872 (2016).
- De Rosa, I. M., Kenny, J. M., Puglia, D., Santulli, C. & Sarasini, F. Morphological, thermal and mechanical characterization of okra (*Abelmoschus esculentus*) fibres as potential reinforcement in polymer composites. *Composite Science Technology* **70**, 116–122 (2010).
- Bessadok, A., Marais, S., Roudesli, S., Lixon, C. & Métayer, M. Influence of chemical modifications on water-sorption and mechanical properties of Agave fibres. *Composite, Part A* **39**, 29–45 (2008).
- Adel, A. M., Abd El-Wahab, Z. H., Ibrahim, A. A. & Al-Shemy, M. T. Characterization of microcrystalline cellulose prepared from lignocellulosic materials. Part I. Acid catalyzed hydrolysis. *Bioresource Technology* **101**, 4446–4455 (2010).

28. Saleh, T. A., Al-Shalalfeh, M. M. & Al-Saadi, A. A. Graphene Dendrimer-stabilized silver nanoparticles for detection of methimazole using Surface-enhanced Raman scattering with computational assignment. *Scientific reports* **6**, 32185 (2016).
29. Saleh, T. A. & Gupta, V. K. Processing methods, characteristics and adsorption behavior of tire derived carbons: a review. *Advances in colloid and interface science* **211**, 93–101 (2014).
30. Saleh, T. A., Rachman, I. B. & Ali, S. A. Tailoring hydrophobic branch in polyzwitterionic resin for simultaneous capturing of Hg (II) and methylene blue with response surface optimization. *Scientific Reports* **7**, 4573 (2017).
31. Roy, S. & Das, P. K. Antibacterial hydrogels of amino acid-based cationic amphiphiles. *Biotechnology and Bioengineering* **100**(4), 756–764 (2008).
32. Vadivelan, V. & Kumar, K. V. Equilibrium, kinetics, mechanism, and process design for the sorption of methylene blue onto rice husk. *Journal of Colloid Interface Science* **286**, 90–100 (2005).
33. Singh, K. P., Mohan, D., Sinha, S., Tondon, G. S. & Gosh, D. Color removal from wastewater using low-cost activated carbon derived from agricultural waste material. *Industrial Engineering Chemistry Research* **42**, 1965–1976 (2003).
34. Mouxiou, E., Eleftheriadis, I., Nikolaidis, N. & Tsatsaroni, E. Reactive dyeing of cellulosic fibers: Use of cationic surfactants and their interaction with reactive dyes. *Journal of Applied Polymer Science* **108**, 1209–1215 (2008).
35. Nebojša, R. & Ivanka, R. Cationic Modification of Cotton Fabrics and Reactive Dyeing Characteristics. *Journal of Engineered Fibers and Fabrics* **7**(4), 113–121 (2012).
36. Jabli, M., Emna, G., Nouha, S. & Mohamed, H. Almond shell waste (*Prunus dulcis*): Functionalization with [dimethyldiallyl-ammonium-chloride-diallylamin-co-polymer] and chitosan polymer and its investigation in dye adsorption. *Journal of Molecular Liquids* **240**, 35–44 (2017).
37. Hassen, A., Jabli, M. & Hatem, M. Synthesis, characterization of hydroxyapatite-lambda carrageenan, and evaluation of its performance for the adsorption of methylene blue from aqueous suspension. *Journal of Applied Polymer Science* **134**(40), 1–9 (2017).
38. EL-Mekkawi, D. M., Ibrahim, F. A. & Selim, M. M. Removal of methylene blue from water using zeolites prepared from Egyptian kaolins collected from different sources. *Journal of Environmental Chemical Engineering* **4**(2), 1417–1422 (2016).
39. Rahimdokht, M., Pajootan, E. & Arami, M. Central composite methodology for methylene blue removal by *Elaeagnus angustifolia* as a novel biosorbent. *Journal of Environmental Chemical Engineering* **4**(2), 1407–1416 (2016).
40. Makrigianni, V., Giannakas, A., Deligiannakis, Y. & Konstantinou, I. Adsorption of phenol and methylene blue from aqueous solutions by pyrolytic tire char: Equilibrium and kinetic studies. *Journal of Environmental Chemical Engineering* **3**, 574–582 (2015).
41. Mittal, A., Mittal, J., Malviya, A. & Gupta, V. K. Removal and recovery of Chrysoidine Y from aqueous solutions by waste materials. *Journal of Colloid and Interface Science* **344**, 497–507 (2010).
42. Gupta, V. K. & Saleh, T. A. Sorption of pollutants by porous carbon, carbon nanotubes and fullerene-An overview. *Environmental science and pollution research* **20**, 2828–2843 (2013).
43. Gupta, V. K. *et al.* Adsorptive removal of dyes from aqueous solution onto carbon nanotubes: a review. *Advances in Colloid and Interface Science* **193**, 24–34 (2013).
44. Saleh, T. A. & Gupta, V. K. Synthesis and characterization of alumina nano-particles polyamide membrane with enhanced flux rejection performance. *Separation and purification technology* **89**, 245–251 (2012).
45. Gupta, V. K. & Saleh, T. A. Characterization of the bonding interaction between alumina and nanotube in MWCNT/alumina composite. *Current Nanoscience* **8**(5), 739–743 (2012).

## Acknowledgements

The authors are grateful to Direction Générale de la Recherche Scientifique of the Tunisian Ministry of Higher Education and Scientific Research for financial support. TA Saleh would like to acknowledge the support and fund provided by King Fahd University of Petroleum & Minerals (KFUPM) through Project No. IN131053 under the Deanship of Research.

## Author Contributions

M.J. contributed to the experimental work, characterization, and T.A.S. contributed to the work discussion and developed the manuscript and review the final article, N.S. contributed to the experimental work, N.T. contributed to the experimental work, R.K. contributed to the experimental work.

## Additional Information

**Supplementary information** accompanies this paper at <https://doi.org/10.1038/s41598-017-14327-7>.

**Competing Interests:** The authors declare that they have no competing interests.

**Publisher's note:** Springer Nature remains neutral with regard to jurisdictional claims in published maps and institutional affiliations.



**Open Access** This article is licensed under a Creative Commons Attribution 4.0 International License, which permits use, sharing, adaptation, distribution and reproduction in any medium or format, as long as you give appropriate credit to the original author(s) and the source, provide a link to the Creative Commons license, and indicate if changes were made. The images or other third party material in this article are included in the article's Creative Commons license, unless indicated otherwise in a credit line to the material. If material is not included in the article's Creative Commons license and your intended use is not permitted by statutory regulation or exceeds the permitted use, you will need to obtain permission directly from the copyright holder. To view a copy of this license, visit <http://creativecommons.org/licenses/by/4.0/>.

© The Author(s) 2017